

# Study on Molecular Mechanism of Benzo (a) pyrene on CMA by HSP90 $\alpha$ and HIF-1 $\alpha$

**Shasha Zhang** (✉ [1039345330@qq.com](mailto:1039345330@qq.com))

Inner Mongolia Medical University

**Tingting Liu**

Inner Mongolia Medical University

**Qi Chen**

Inner Mongolia Medical University

**Min Su**

Inner Mongolia Medical University

**Tuya Bai**

Inner Mongolia Medical University

**Mengdi Zhang**

Inner Mongolia Medical University

**Yuxia Hu**

Inner Mongolia Medical University

**Jun Li**

Inner Mongolia Medical University

**Fuhou Chang**

Inner Mongolia Medical University

---

## Research Article

**Keywords:** A549, HSP90 $\alpha$ , HIF-1 $\alpha$ , BaP, Molecular chaperone autophagy

**Posted Date:** August 10th, 2021

**DOI:** <https://doi.org/10.21203/rs.3.rs-763034/v1>

**License:**   This work is licensed under a Creative Commons Attribution 4.0 International License.

[Read Full License](#)

---

# Abstract

**OBJECTIVE:** The effects of benzo (a) pyrene (BaP) on molecular chaperone autophagy (CMA) through heat shock protein 90 (HSP90) and hypoxia inducible factor-1 (HIF-1) were studied by RNA interference and subcutaneous tumor formation technique in nude mice.

**METHODS:** 40 nude mice inoculated with the shHSP90 A549 cell line under the armpits of the forelimbs were divided into 4 groups, 1.80 mg/kg/d BaP-corn oil solution was intragastrically administered for 60 days (except the Control group), and the growth of nude mice and transplanted tumors was recorded curve. The size and morphological changes of tumors were observed by small animal imaging technique and HE staining method. qPCR, Western blot and Immunohistochemistry were used to detect the expression of HSP90, HSC70 and Lamp-2A. A549 cells were treated with 0.1 μmol/L, 1 μmol/L and 10 μmol/L BaP for 24h, EPO, HIF-1 concentration and HIF-1 protein expression were detected by Elisa and Western blot; A549 cells were treated with 10 μmol/L BaP and added HIF-1 inhibitor 24h, qPCR, Western blot and Immunofluorescence method were used to detect the expression of HSP90, HSC70 and Lamp-2A.

**RESULTS:** BaP can reduce silence HSP90 the weight of nude mice and transplanted tumors ( $P < 0.01$ ); BaP can reduce silence HSP90 the expression of HSP90, HSC70, Lamp-2A mRNA and protein in transplanted tumor tissues ( $P < 0.05$ ); BaP has no significant difference in the organization structure of silence HSP90 and non-silence HSP90; BaP can reduce the total number of bioluminescence photons of silence HSP90 transplanted tumors ( $P < 0.01$ ). 10 μmol/L BaP can increase the concentration of EPO and HIF-1 and the expression of HIF-1 protein in A549 cells ( $P < 0.05$ ); and after adding HIF-1 inhibitors treat A549 cells, HSP90, HSC70, Lamp-2A mRNA and protein expression were decreased ( $P < 0.05$ ), and the fluorescence intensity of HSP90 was decreased.

**CONCLUSIONS:** BaP can promote the growth of transplanted tumor in nude mice, while the growth of transplanted tumor in nude mice is inhibited shHSP90. BaP promotes the occurrence of CMA by promoting the expression of HSP90 and HIF-1, which are important regulatory genes for BaP to activate CMA.

## Introduction

Autophagy is a lysosome-dependent protein degradation pathway, which maintains the balance and homeostasis of the internal environment through the degradation and recycling of proteins and damaged organelles, which is a highly conservative process in eukaryote evolution.<sup>1</sup> Autophagy can be divided into macroautophagy, microautophagy and molecular chaperone autophagy (CMA) according to the different ways of transport of degradable substances to lysosomes.<sup>2</sup> CMA is a kind of selective autophagy. Firstly, the recognition process of substrate protein occurs in the cytoplasm. The pentapeptide motif KFERQ in the amino acid sequence binds to the heat shock protein 70 (HSC70) with molecular weight 70KDa. When the substrate protein binds to the corresponding molecular chaperone, it further binds to the cytoplasmic

tail of the receptor lysosome associated membrane protein 2 (Lamp-2A) on the surface of the lysosome. When the substrate is transported into the lysosomal cavity, Lamp-2A will quickly dissociate from the transport complex to form a monomer, and the substrate can be degraded by the lysosome.<sup>3</sup> Studies have found that autophagy is closely related to the occurrence and development of lung cancer, which plays different roles in suppressing and promoting cancer in the early and late stages of tumorigenesis. On the one hand, in the early stage of tumorigenesis, autophagy maintains cell stability and inhibits its transformation into tumor cells by inhibiting inflammation, maintaining genomic stability, promoting the senescence of damaged cells and inhibiting the accumulation of p62, and inhibits its transformation into tumor cells. In the late stage of tumorigenesis, the initial tumor cells have been formed, and this process is more likely that the initial tumor cells continue to grow and transform in a relatively barren environment, and finally form a tumor, in this process, autophagy promotes the survival and proliferation of tumor cells mainly by helping tumor cells resist internal and external pressure and regulating the vigorous metabolism of tumor cells.<sup>4-6</sup> Heat shock protein 90 (HSP90) is a key factor for eukaryotic cells to regulate protein homeostasis under physiological and stress conditions,<sup>7,8</sup> HSP90 can recognize the unfolded region of substrate protein in the process of CMA and prevent the formation of polymer during the transfer of molecular chaperone-substrate complex to Lamp-2A on lysosomal membrane, and plays an important role in the CMA process.<sup>9</sup> Studies have found that the expression of HSP90 is increased in a variety of cancer tissues.<sup>10,11</sup> HSP90 chaperones are necessary for the conformational maturation and stability of a variety of oncogenic kinases, which can drive signal transduction and proliferation of lung cancer cells.<sup>12</sup> Therefore, HSP90 can promote the occurrence and development of lung cancer.

The first kind of carcinogens found in tobacco smoke include polycyclic aromatic hydrocarbons (PAHs). Which has the characteristics of lipophilicity, refractory, bioaccumulation, cytotoxicity, mutagenicity and carcinogenicity.<sup>13,14</sup> Benzo[a]pyrene (BaP) is the most common PAHs, and BaP exposure is closely related to the incidence of lung cancer.<sup>15</sup> As we all know, BaP is a classic exogenous ligand of Aryl hydrocarbon receptor (AhR). In the absence of ligand, AhR and HSP90, hepatitis B virus X-related protein 2 (XAP2) and p23 protein exist in the cytoplasm as a complex. These auxiliary factors stabilize the ligand state of AhR and prevent its degradation. When BaP and AhR bind, HSP90, p23, XAP2 and AhR are separated, and AhR forms a dimer with Aryl receptor nuclear translocator (ARNT/HIF-1 $\beta$ ), which is transferred to the nucleus and then induces the expression of cytochrome P450 (1A1, 1A2, 1B1). Its function is mainly involved in the detoxification of aromatic hydrocarbons, while HSP90 is free in the cytoplasm.<sup>16,17</sup>

Hypoxia-inducible factor-1 $\alpha$  (HIF-1 $\alpha$ ) is the regulatory subunit of the transcription factor HIF-1, mainly involved in oxygen sensing and promoting cell survival under hypoxic conditions.<sup>18,19</sup> HIF-1 is a heterodimer composed of  $\alpha$  and  $\beta$  subunits. The activity of HIF-1 transcription complex is regulated by HIF-1 $\alpha$  subunit in oxygen-dependent processes after translation. In the presence of oxygen, HIF-1 $\alpha$  is hydroxylated by proline hydroxylase (PHDs), which binds to the Von hippel-lindau protein (pVHL) and E3 ubiquitin ligase complex, resulting in the proteasome of HIF-1 $\alpha$  degradation. However, under hypoxia, HIF-1 $\alpha$  avoids the degradation pathway, allowing it to be transported to the nucleus to form a transcriptionally

active HIF-1 complex.<sup>20</sup> In the tumor hypoxic microenvironment, HIF-1 $\alpha$  is up-regulated and stabilized, resulting in up-regulated expression of genes related to glycolysis, angiogenesis and cell survival, thus promoting tumor growth.<sup>21</sup> Studies have shown that HIF-1 $\alpha$  can interact with HSP90, the stability of HIF-1 $\alpha$  is regulated by HSP90, and newly synthesized HIF-1 $\alpha$  can be stabilized by HSP90 to prevent its degradation. Drugs related to HSP90 can inhibit a variety of cancer pathways including HIF-1.<sup>22</sup> Moreover, hypoxia, as a stress response, can also induce autophagy. Studies have shown that overexpression of HSC70 or Lamp-2A leads to a significant decrease in HIF-1 $\alpha$  levels, while knockout of HSC70 or Lamp-2A has the opposite effect.<sup>23</sup> However, the effect of HIF-1 $\alpha$  on CMA-related gene Lamp-2A has not been reported. In order to further clarify the effect of BaP on CMA through HSP90 $\alpha$  and HIF-1 $\alpha$ , this experiment used nude mice tumor formation experiment to verify the silence of HSP90 $\alpha$ , and BaP was administered to the stomach to observe its effect on the tumor, BaP and HIF-1 $\alpha$  inhibitors treat A549 cells, explore the effect of BaP on CMA, and provide a theoretical basis for finding the target of lung cancer treatment.

## Materials And Methods

### Chemicals

Lentivirus pMT470, HSP90 knockdown Luc lentivirus pLVE2620 (Sangon Biotech); Lipfectamine 3000 Liposome transfection Kit (Thermo Company, USA); DH5 $\alpha$  competent cells, LB liquid medium (Thermo Company, USA); ethanol absolute, isopropanol, glycerol, anhydrous calcium chloride (Shanghai Aladdin biochemical Technology Co., Ltd.); Trypsin, penicillin, dimethylsulfoxide, ethidium bromide (Wuhan Boster Biological Technology Co., Ltd.); BaP (Sigma, USA); HSP90 $\alpha$  Antibody, HSC70 Antibody, Lamp-2A Antibody, HIF-1 $\alpha$  Antibody, GAPDH Antibody, HRP-conjugated goat anti-rabbit IgG (abcam, USA); RNA simple Total RNA Kit (Tiangen biotech (Beijing) Co., Ltd.); Rever Tra Ace qPCR RT Kit, Fluorescence quantitative detection (SYBR Green) kit (TOYOBO, Japan); HIF-1 inhibitor BAY87-2243, DAPI staining solution, RIPE lysate, RIPA lysate (Beyotime); HE dye (Shanghai Bogoo Biotechnology Co., Ltd.); Human EPO Elisa kit Human HIF-1 $\alpha$  Elisa kit (Shanghai Yili Biotechnology Co., Ltd.).

### Animals

40 BALB/C nude mice (male, 6–8 weeks, 18-22g); provided by Sipeifu Beijing Biotechnology Co., Ltd., BALB/C mice production license: SCXK (Beijing) 2019-0010, raised in the New Drug Safety Evaluation Research Center of Inner Mongolia Medical University (barrier environment, temperature 20–26°C, humidity 40% Rue 70%). All animal experiments are approved by the Animal Management Association of Inner Mongolia Medical University and meet the relevant requirements of the Ethical Committee of Inner Mongolia Medical University.

### Cell culture

Human lung adenocarcinoma cell line A549, from the cell bank of Chinese Academy of Sciences. The DMEM medium containing 100IU/mL penicillin, 100IU/mL streptomycin and 10% fetal bovine serum was

cultured at 37 °C in 5%CO<sub>2</sub> incubator.

## Stable transfection of A549 cells

The cell density reached 80%~90%, and the cells were transfected with pMT470 and pLVE2620 lentivirus according to MOI = 30. After 48h, the cells were replaced with a selection medium containing 2µg/mL puromycin, and the fluorescence of the cells was observed. After 2 weeks, the cells infected with the virus fluid have formed a clonal population. The culture medium containing puromycin was replaced every 24h, and the cells were passaged and collected.

## QPCR

RNA isolation, cDNA synthesis, quantitative real-time PCR and primer sequences were described previously.(Table 1, 2)

Table 1  
primer sequence

Gene	Species	Primer sequence(5'–3')
<i>HSP90</i>	Human	Forward primer 5'-GGATCCAGTCCTGAGGAAACCCAGACC-3'
		Reverse primer 5'-TCTAGATTAGTCTAGTTCTTCCATGCG-3'
<i>Lamp-2A</i>	Human	Forward primer 5'-TATGTGCAACAAAGAGCAGA-3'
		Reverse primer 5'- CAGCATGATGGTGCTTGAGA-3'
<i>HSC70</i>	Human	Forward primer 5'-GCCAACAAGATCACCATCAC-3'
		Reverse primer 5'-GCTCAAACCTCGTCCTTCTC-3'
<i>HIF-1</i>	Human	Forward primer 5'-GTGGTGGTTACTCAGCACTTTT-3'
		Reverse primer 5'-TCCGTCCCTCAACCTCTCAG-3'
<i>GAPDH</i>	Human	Forward primer 5'-GGATGTCCACGTCACACTTC-3'
		Reverse primer 5'-CACTCTTCCAGCCTTCCTTC-3'

Table 2  
primer sequence

Gene	Species	Primer sequence(5'—3')
<i>HSP90</i>	Mouse	Forward primer 5'-GTTACGAGAGCCTGACGGAC-3'
		Reverse primer 5'-ACAATGGTCAGGGTTCGGTC-3'
<i>Lamp-2A</i>	Mouse	Forward primer 5'-AGAGCGTTTCAGATCAACACCT-3'
		Reverse primer 5'-CGCTATGGGCACAAGGAAGT-3'
<i>HSC70</i>	Mouse	Forward primer 5'-GCGTACCTCGGAAAGGCAA-3'
		Reverse primer 5'-ATAGCAGCAGCAGTTGGTTCA-3'
<i>GAPDH</i>	Mouse	Forward primer 5'-CTACCTCATGAAGATCCTGACC-3'
		Reverse primer 5'-CACAGCTTCTCTTTGATGTCAC-3'

## Western blot

The cells were collected, washed 3 times with PBS, and the cells were lysed with RIPA lysis to extract protein. Separate the protein by SDS-PAGE electrophoresis, transfer it to PVDF membrane, incubate the HSP90 Antibody, HSC70 Antibody, Lamp-2A Antibody, HIF-1 Antibody overnight at 4°C, wash the membrane 3 times with TBST, incubated for 1h at room temperature with HRP-conjugated goat anti-rabbit IgG, immunolabelled bands were visualized using Immobilon chemiluminescent HRP substrate according to manufacturer instructions. The results of the western blot were quantified by densitometric scanning of immunoblots with Odyssey CLx. The densitometric analysis of the selected proteins was performed in relation to a reference protein (GAPDH), providing data presented as arbitrary optical density units.

## Small Animal Imaging Technology

40 nude mice were adaptively fed with ordinary feed for a week and then randomly divided into 4 groups: shControl group, shControl + BaP group, shHSP90 group, shHSP90+BaP group, 10 animals in each group. The experimental group was given BaP-corn oil solution 1.80 mg/kg/d by gavage, and the control group was given corn oil solution by gavage. Count the cells with a hemocytometer, and finally resuspend them in a certain volume of PBS to make the concentration of the cell suspension  $1 \times 10^7$  cells/mL. A suspension containing  $2 \times 10^6$  cells was injected into the right axilla of nude mice. The experiment process was carried out in the SPF barrier environment. Nude mice were raised two weeks after injection until tumors were visible to the naked eye. Measure the body weight and the length and short diameter of the tumor body of the nude mouse every 10 days, and calculate the tumor volume of the nude mouse.<sup>24</sup> After six consecutive measurements (60 days), in vivo imaging detection and animal sampling were carried out to detect the related indexes.

8 weeks after the establishment of transplanted tumor model of nude mice, the nude mice in isoflurane equipment to anesthetize and place in the in vivo imager. The emission wavelength was 560 nm, the excitation wavelength was 480 nm, and the exposure time was 1s. The volume and photon values were measured and images were collected. A pseudo-color scale is used to indicate the photon count of each mouse.

## HE staining

Fasting for 12h before taking the material and weighing, anaesthetized by 0.1mL/10g intraperitoneal injection of 10% paraformaldehyde, 75% ethanol disinfected the subaxillary skin of nude mice, and the tumor tissue of nude mice was stripped off, weighed, cut off half of the tumor tissue of nude mice, then put the tumor tissue of nude mice into a wide mouth bottle containing 4% paraformaldehyde and fixed at 4°C for a week. The fixed tumor tissue of nude mice was cut into the size of 1.0cm×1.0cm×0.3cm, and the pathological sections were prepared, hematoxylin-eosin staining and observation.

## Immunohistochemical

The prepared sections were analyzed by immunohistochemistry and pictures were collected using a Leica microscope. The collected pictures were quantified using the HALO V 3.1 image analysis platform (Indica Labs, Albuquerque, NM, USA).

## ELISA

A549 cells with different concentrations of BaP (0.1μmol/L, 1μmol/L, 10μmol/L) for 24h, the contents of EPO and HIF-1α were detected by ELISA kit.

## Immunofluorescence

A549 cells were pread in a 6-well plate, divided into Control group, BaP group (1μmol/L), BAY87-2243 group (100nmol/L),<sup>25</sup> BaP + BAY87-2243 group after 24h, immunofluorescence method was used to detect the fluorescence intensity of HSP90α.

## Statistics

All statistical tests were performed using the SPSS 20.0. The data is expressed by  $\bar{X} \pm S$ , and the data is in accordance with the normal distribution by Shapiro-Wilk (S-W) test, and the data comparison between multiple groups is tested by one-way-ANOVA.  $P < 0.05$  means the difference is statistically significant. Graphpad Prism analysis results.

## Results

### *Stable transfection of A549 cell line*

48h after lentivirus transfection into lung cancer A549 cells, the lentivirus transfection efficiency of A549 cells was observed by fluorescence microscope and counted under ordinary light and fluorescence

microscope. Under the white light field, A549 cells in shControl group and shHSP90 group were evenly distributed under the blank, and the cells were in good condition. In the fluorescent group, the number of fluorescent cells was more than shControl, but the fluorescence intensity was not strong. The reason may be that the existence of Luciferase affected the expression of green fluorescent protein (GFP). Therefore, this experiment is followed by qPCR and Western blot verification. The transfection efficiency is more than 90%, and the silencing effect is good, which can be used in subsequent experiments. (Figure 1)

### ***QPCR***

Compared with the shControl group, the expression of HSP90 $\alpha$  in the shHSP90 $\alpha$  group was decreased ( $P<0.05$ ) (Figure 2C). According to the results of HSP90 $\alpha$  mRNA expression after transfection, it can be concluded that transfection of recombinant plasmid shHSP90 $\alpha$  can effectively reduce HSP90 $\alpha$  mRNA expression with an efficiency of about 70%, so A549 cell was selected for subsequent experiments.

### ***Western blot***

After 24h of transfection, compared with the shControl group, the expression of HSP90 $\alpha$  protein in the shHSP90 $\alpha$  group was decreased ( $P<0.05$ ) (Figure 2A, 2B).

### ***Small Animal Imaging Technology***

After 12d of 40 nude mice, tumors formed in each group (the tumor volume was about 100mm<sup>3</sup>) (Figure 3A), 2 died in the shControl group (transfection blank plasmid group), 3 died in the shControl+BaP group, 1 died in the shHSP90 $\alpha$  group, and 2 died in the shHSP90 $\alpha$ +BaP group during the breeding process. The rest of the nude mice had normal eating and drinking, and no adverse reactions such as slow activity and diarrhea. Measure the length and short diameter of the tumor and the weight of the nude mice every 10d and observe the changes in its volume and weight, and draw the growth curve (Figure 3C, 3D). Compared with the shControl group, the volume and weight of transplanted tumors in the shControl+BaP group were increased ( $P<0.01$ ); compared with the shControl+BaP group, the volume and weight of the shHSP90 $\alpha$ +BaP group were decreased ( $P<0.01$ ). The stronger the fluorescence signal intensity of tumor cells, the greater the number of tumor cells, and the larger the tumor. Compared with shControl group, the total bioluminescence photon number of transplanted tumors in the shControl+BaP group was increased ( $P<0.01$ ); compared with shControl+BaP group, the total bioluminescence photon number in the shHSP90 $\alpha$ +BaP group was decreased ( $P<0.01$ ) (Figure 3B, 3E). It shows that in vivo experiments, shHSP90 $\alpha$  can eliminate the role of BaP in promoting the growth of transplanted tumors in nude mice.

### ***HE staining***

Different degrees of necrosis were observed in the tumors of each group. The shcontrol group had the largest area of necrosis with large sheet necrosis, while the shcontrol+BaP group had a smaller necrosis area. Deep staining, nuclear pyknosis, disordered cell arrangement, in line with the pathological



characteristics of cancer cells. There was no significant difference in the tissue structure between the shHSP90 $\alpha$  group and shHSP90 $\alpha$ +BaP group (Figure 4).

### ***Expression of CMA-related mRNA and protein in transplanted tumors***

The mRNA and protein expression of HSP90 $\alpha$ , HSC70 and Lamp-2A in transplanted tumor tissues of nude mice was measured to explore the role of HSP90 $\alpha$  in BaP-induced CMA-related mRNA and protein. Compared with the shControl group, the expressions of HSP90 $\alpha$ , HSC70 and Lamp-2A mRNA and protein in the transplanted tumor tissues of the shControl+BaP group were increased ( $P<0.01$ ,  $P<0.01$ ,  $P<0.05$ ); compared with the shControl+BaP group, the shHSP90 $\alpha$ +BaP group HSP90 $\alpha$ , HSC70 and Lamp-2A mRNA and protein expression decreased ( $P<0.01$ ,  $P<0.01$ ,  $P<0.05$ ) (Figure 5). The results show that at the mRNA and protein level, BaP can promote the expression of CMA-related mRNA and protein, and shHSP90 $\alpha$  can eliminate the role of BaP in promoting the expression of CMA-related mRNA and protein.

### ***Immunohistochemical***

The protein expressions of HSP90 $\alpha$ , HSC70, and Lamp-2A in the transplanted tumor tissues of nude mice were measured, and the pictures were quantified. Strong positive region is red, moderate positive region is orange, and weak positive region is yellow. Compared with the shControl group, HSP90 $\alpha$ , HSC70 and Lamp-2A in the shControl+BaP group accounted for higher proportions of strong positive region ( $P<0.05$ ); compared with the shControl+BaP group, HSP90 $\alpha$ , HSC70, and Lamp-2A in the shControl+BaP group accounted for the ratio decreased ( $P<0.05$ ) (Figure 6~9, Table 3~5). The results show that at the protein level, BaP can promote the expression of CMA-related genes, while silencing HSP90 $\alpha$  can eliminate the role of BaP in promoting CMA-related gene expression, which is consistent with the results of qPCR and Western blot.

TABLE 3. Proportion of HSP90 $\alpha$  positive degree

HSP90 $\alpha$ positive degree  Proportion(%)  Group	shControl	shControl+BaP	shHSP90 $\alpha$	shHSP90 $\alpha$ +BaP
	shControl	shControl	shControl	shControl
	shControl+BaP	shControl+BaP	shControl+BaP	shControl+BaP
	shHSP90 $\alpha$	shHSP90 $\alpha$	shHSP90 $\alpha$	shHSP90 $\alpha$
	shHSP90 $\alpha$ +BaP	shHSP90 $\alpha$ +BaP	shHSP90 $\alpha$ +BaP	shHSP90 $\alpha$ +BaP
%Weak Positive Region	46.06 $\pm$ 5.51	19.9 $\pm$ 1.15	48.09 $\pm$ 7.21	35.33 $\pm$ 4.58
%Moderate Positive Region	44.53 $\pm$ 6.03	49.09 $\pm$ 5.51	43.37 $\pm$ 6.43	55.61 $\pm$ 6.11
%Strong Positive Region	9.4 $\pm$ 10.12	31 $\pm$ 6.08*	8.54 $\pm$ 3.06	9.05 $\pm$ 1.53 <sup>#</sup>

TABLE 4. Proportion of HSC70 positive degree

HSC70 positive degree  Proportion(%)  Group	shControl	shControl+BaP	shHSP90 $\alpha$	shHSP90 $\alpha$ +BaP
	shControl	shControl	shControl	shControl
	shControl+BaP	shControl+BaP	shControl+BaP	shControl+BaP
	shHSP90 $\alpha$	shHSP90 $\alpha$	shHSP90 $\alpha$	shHSP90 $\alpha$
	shHSP90 $\alpha$ +BaP	shHSP90 $\alpha$ +BaP	shHSP90 $\alpha$ +BaP	shHSP90 $\alpha$ +BaP
%Weak Positive Region	26.38 $\pm$ 8.52	11.53 $\pm$ 0.95	47.44 $\pm$ 2.59	29.28 $\pm$ 3.63
%Moderate Positive Region	37.51 $\pm$ 5.03	25.12 $\pm$ 3.02	37.04 $\pm$ 3.21	42.89 $\pm$ 3.58
%Strong Positive Region	36.11 $\pm$ 13.38	63.35 $\pm$ 2.89*	15.52 $\pm$ 2.7	27.83 $\pm$ 7.09 <sup>##</sup>

TABLE 5. Proportion of Lamp-2A positive degree

Lamp-2A	shControl	shControl+BaP	shHSP90	shHSP90+BaP
Positive degree	shControl	shControl	shControl	shControl
degree	shControl+BaP	shControl+BaP	shControl+BaP	shControl+BaP
Proportion(%)	shHSP90	shHSP90	shHSP90	shHSP90
Group	shHSP90+BaP	shHSP90+BaP	shHSP90+BaP	shHSP90+BaP
%Weak Positive Region	15.23±3.78	7.57±2.65	11.67±1.53	8.09±3
%Moderate Positive Region	70.84±5.99	35.09±5.03	59.03±7.64	61.28±10.02
%Strong Positive Region	13.93±4.46	57.34±7.64**	29.3±6.11	30.63±13.01#

Note: \* means compared with shControl group  $P < 0.05$ , \*\*  $P < 0.01$ ; # means compared with shControl+BaP group  $P < 0.05$ , ##  $P < 0.01$ .

### **ELISA**

Different concentrations of BaP were detected on the expression of erythropoietin (EPO) and HIF-1 $\alpha$ , and the BaP would cause the A549 cells hypoxic environment. The results show that the expression of the BaP concentration is 10  $\mu\text{mol/L}$ , the expression of EPO and HIF-1 $\alpha$  were increased ( $P < 0.01$ ,  $P < 0.05$ ) (Figure 9A, B). The experimental results show that the BaP can cause A549 cells to hypoxia when 10  $\mu\text{mol/L}$ . The BaP concentration is selected 10  $\mu\text{mol/L}$ . Western blot was used to detect the influence of different concentrations of BaP on HIF-1 $\alpha$  protein. When the concentration of BaP was 10  $\mu\text{mol/L}$ , compared with the control group, the expression of HIF-1 $\alpha$  protein was increased ( $P < 0.05$ ) (Figure 10C, D). The results indicate that BaP may cause hypoxia in A549 cells, thereby increasing the expression of HIF-1 $\alpha$ , which is concentration-dependent.

### **Immunofluorescence**

The green fluorescence represents the expression of HSP90 $\alpha$  protein, and the blue represents the nucleus. Compared with the Control group, the fluorescence intensity of HSP90 $\alpha$  in the BaP group increased. When the HIF-1 $\alpha$  inhibitor was added, compared with the BaP group the fluorescence intensity of HSP90 $\alpha$  was decreased (Figure 11). The experimental results show that at the protein level, inhibition of HIF-1 $\alpha$  can eliminate the HSP90 $\alpha$  expression of BaP in A549 cells.

### **Expression of CMA-related mRNA and protein in A549 cells**

The mRNA and protein expressions of HSP90 $\alpha$ , HSC70, Lamp-2A, and HIF-1 $\alpha$  in different groups of A549 cells were measured, and the role of HIF-1 $\alpha$  in BaP-regulated CMA-related mRNA and proteins level. Compared with the Control group, the expression of HSP90 $\alpha$ , HSC70, Lamp-2A, HIF-1 $\alpha$  mRNA and protein in the BaP group increased ( $P<0.05$ ). When HIF-1 $\alpha$  inhibitor was added, compared with the BaP group, HSP90 $\alpha$ , HSC70, Lamp-2A, HIF-1 $\alpha$  mRNA and protein expression was decreased ( $P<0.05$ ) (Figure 12). The experimental results show that at the gene and protein level, inhibiting HIF-1 $\alpha$  can partially eliminate CMA-related genes the expression of BaP in A549 cells.

## Discussion

This study used nude mice tumor experiments to prove that HSP90  $\alpha$  plays a very important role in the development of tumors and CMA. At the animal level, protein and mRNA levels prove that BaP can promote the expression of CMA-related genes HSP90, HSC70 and Lamp-2A, and silencing HSP90 $\alpha$  can partially eliminate the up-regulation of BaP on the expression of CMA-related genes in A549 cells. The in vitro experiments in the early stage of the project are the same.<sup>26</sup> This study also proves that BaP can cause the tumor hypoxic microenvironment to increase HIF-1 $\alpha$  and promote the occurrence of CMA, and at the cellular level, after inhibiting HIF-1 $\alpha$  in A549 cells, the expression of CMA-related genes is down-regulated.

HSP90 is a lysosomal associated partner, has been shown to be co-located on the lysosomal membrane, which can interact with Lamp-2A on the lysosomal membrane, with autophagy inhibitor 17-dimethylaminoethyl lysomycin-2a degradation of LAMP-2A is faster than the peroxymycin (17DMAG) treated. Lamp-2A organizes a dynamic multimeric complex to participate in the process of CMA. HSP90 is essential to ensure the stability of Lamp-2A in the dynamics of multi-molecular complexes, thereby stabilizing the process of CMA.<sup>7</sup> During the CMA, with the help of cytoplasmic chaperones and cofactors, HSC70 can identify about 40% of mammalian protein. HSC70 degrades proteins towards the proteasome or lysosome. HSC70 plays a decisive role in CMA. It is a limiting factor for protein translocation and also participates in the processing of targeted proteins through lysosomal forms.<sup>27</sup> Therefore, HSP90 mainly plays a role in stabilizing Lamp-2A in the process of CMA, HSC70 is responsible for recognizing the substrate protein, thus ensuring the smooth progress of the CMA process, inducing the expression of CMA-related genes, and HSP90 deletion results in a decrease in CMA gene expression.

EPO is an essential survival and growth factor for red blood cells. EPO is mainly produced in the kidney, and HIF can induce EPO gene expression. HIF family (HIF-1,2 and 3), the main representative of which is HIF-1, which consists of an O<sub>2</sub> unstable  $\alpha$  subunit and a constant nuclear  $\beta$  subunit. Under normal oxygen conditions,  $\alpha$ -oxyfamic acid and Fe<sup>2+</sup> dependent HIF-specific double oxygenase then after prolineyl and asparagin hydroxylation, the  $\alpha$ -subunit of HIF is inactivated and degraded. Under oxygen conditions, HIF-1 will not be degraded, so under hypoxia, HIF-1 can induce the expression of EPO.<sup>28,29</sup> The hypoxic microenvironment is ubiquitous in many solid tumors and is resistant to tumor treatment methods such as conventional chemotherapy, radiotherapy, newly developed molecular targeted therapies and

immunotherapy, which also demonstrates that BaP promotes cancer occurrence. Mechanisms, studies have shown that HIF-1 $\alpha$  interacts with CMA-related genes HSC70 and Lamp-2A. Overexpression of HSC70 or Lamp-2A reduces the protein level of HIF-1 $\alpha$ ,<sup>23</sup> but the effect of HIF-1 $\alpha$  on CMA has not been reported. In this experiment, the HIF-1 $\alpha$  inhibitor with BaP were used to treat A549 cells. qPCR, western blot and immunofluorescence experiments showed that when HIF-1 $\alpha$  was inhibited, BaP could partially eliminate the expression of CMA-related genes in A549 cells, indicating that BaP can regulate CMA through HIF-1 $\alpha$ , and its mechanism may be caused by hypoxia in A549 cells. The specific mechanism needs to be further studied.

In recent years, various inhibitors of HSP90 and HIF-1 $\alpha$  have been discovered, and HSP90 and HIF-1 $\alpha$  have become targets for the development of new cancer treatments. Many HSP90 and HIF-1 $\alpha$  inhibitors have been developed, some of which are undergoing clinical trials and have certain therapeutic effects on cancer.<sup>30</sup> For example, Chan et al.<sup>31</sup> reported that the HSP90 inhibitor AT13387 can inhibit cell growth, cell migration, tumor spheres and induce cell aging in vitro and in vivo. Unfortunately, due to its minimal effect, it has not been approved for clinical. Therefore, it is imperative to study the interaction network of HSP90 and HIF-1 $\alpha$  to find more effective anti-cancer targets.

## Abbreviations

benzo (a) pyrene (BaP)

molecular chaperone autophagy (CMA)

hypoxia inducible factor-1 (HIF-1)

heat shock protein (HSC70)

lysosome associated membrane protein 2 (Lamp-2A)

heat shock protein 90 (HSP90)

polycyclic aromatic hydrocarbons (PAHs)

aryl hydrocarbon receptor (AhR)

hepatitis B virus X-related protein 2 (XAP2)

aryl receptor nuclear translocator (ARNT/HIF-1 $\beta$ )

proline hydroxylase (PHDs)

von hippel-lindau protein (pVHL)

green fluorescent protein (GFP)

erythropoietin (EPO)

## Declarations

Ethics approval and consent to participate

The full text or part of the paper has not been submitted or published elsewhere. The paper will not be submitted elsewhere until the procedures of the journal editorial department are completed. All authors agree to participate.

Consent for publication

All authors agree to publish.

Availability of data and material

All data and material generated or analysed during this study are included in this published article [and its supplementary information files].

Competing interests

No compete of interest.

Funding

This research was supported by the National Natural Science Foundation of China (81760676); the Natural Science Foundation of Inner Mongolia Autonomous Region (2019LH08017); Inner Mongolia Autonomous Region Higher Education Scientific Research Project (NJZY21593).

Authors' contributions

Shasha Zhang, Tingting Liu:Experimental operation; Qi chen, Min Su:Data collection and analysis; Tuya Bai, Yuxia Hu:Thesis drafting; Mengdi Zhang, Fuhou Chang:Put forward the research ideas and design the research scheme; Jun Li:Revision of the final edition of the paper.

Acknowledgements

Thanks to the strong support and help provided by the New Drug Safety Evaluation Research Center and the National Natural Science Foundation of China (81760676), the Natural Science Foundation of Inner Mongolia Autonomous Region (2019LH08017), Inner Mongolia Autonomous Region Higher Education Scientific Research Project (NJZY21593) research fund.

## References

1. Livingston MJ, Dong Z. Autophagy in Acute Kidney Injury[J]. *Seminars in Nephrology*, 2014, 34(1): 17–26.
2. Cerri S, Blandini F. Role of Autophagy in Parkinson's Disease[J]. *Current Medicinal Chemistry*, 2019, 26(20): 3702–3718.
3. Dou J, Su P, Xu C, et al. Targeting Hsc70-based autophagy to eliminate amyloid  $\beta$  oligomers[J]. *Biochem Biophys Res Commun*, 2020, 524: 923–928.
4. Lin L, Baehrecke EH. Autophagy, cell death, and cancer[J]. *Mol Cell Oncol*, 2015, 2 (3): e985913.
5. Nakahira K, Pabon Porras MA, Choi AM. Autophagy in Pulmonary Diseases[J]. *Am J Respir Crit Care Med*, 2016, 194: 1196–1207.
6. Florian H, Schopf, et al. The HSP90 chaperone machinery[J]. *Nature Reviews Molecular Cell Biology*, 2017, 18(6): 345–360.
7. Liao ZZ, Wang B, Liu WJ et al. Dysfunction of chaperone-mediated autophagy in human diseases[J]. *Mol Cell Biochem*, 2021.
8. Liu SS, Li XJ. Regulation of Autophagy in Neurodegenerative Diseases by Natural Products[J]. *Adv Exp Med Biol*, 2020, 1207: 725–730.
9. Bandyopadhyay U, Kaushik S, Varticovski L, et al. The chaperone-mediated autophagy receptor organizes in dynamic protein complexes at the lysosomal membrane[J]. *Mol Cell Biol*, 2008, 28: 5747–63.
10. Vartholomaiou E, Madon-Simon M, Hagmann S, et al. Cytosolic HSP90 $\alpha$  and its mitochondrial isoform Trap1 are differentially required in a breast cancer model[J]. *Oncotarget*, 2017, 8: 17428–17442.
11. Pearl LH. Review: The HSP90 molecular chaperone-an enigmatic ATPase[J]. *Biopolymers*, 2016, 105: 594–607.
12. Bzowska M, Nogieć A, Bania K, et al. Involvement of cell surface 90 kDa heat shock protein (HSP90) in pattern recognition by human monocyte-derived macrophages[J]. *J Leukoc Biol*, 2017, 102: 763–774.
13. Yamaguchi A, Uchida M, Ishibashi H, et al. Potential mechanisms underlying embryonic developmental toxicity caused by benzo[a]pyrene in Japanese medaka (*Oryzias latipes*)[J]. *Chemosphere*, 2020, 242: 125243.
14. Feng BH, Li LJ, Xu HB, et al. PM-bound polycyclic aromatic hydrocarbons (PAHs) in Beijing: Seasonal variations, sources, and risk assessment[J]. *J Environ Sci (China)*, 2019, 77: 11–19.
15. Taghvaei S, Sowlat MH, Hassanvand MS, et al. Source-specific lung cancer risk assessment of ambient PM-bound polycyclic aromatic hydrocarbons (PAHs) in central Tehran[J]. *Environ Int*, 2018, 120: 321–332.
16. Zhou YY, Zhao YA, Xu RY, et al. Study on the AhR signaling pathway and phase II detoxification metabolic enzymes isoforms in scallop *Chlamys farreri* exposed to single and mixtures of PAHs[J]. *Environ Res*, 2020, 190: 109980.

17. Meyer BK, Perdew GH. Characterization of the AhR-HSP90-XAP2 core complex and the role of the immunophilin-related protein XAP2 in AhR stabilization[J]. *Biochemistry*, 1999, 38: 8907–17.
18. Balamurugan K. HIF-1 at the crossroads of hypoxia, inflammation, and cancer[J]. *Int J Cancer*, 2016, 138(5): 1058–66.
19. Mavrofrydi O, Papazafiri P. Hypoxia-inducible factor-1 $\alpha$  increase is an early and sensitive marker of lung cells responding to benzo[a]pyrene[J]. *J Environ Pathol Toxicol Oncol*, 2012, 31: 335–47.
20. Masoud GN, Li W. HIF-1 $\alpha$  pathway: role, regulation and intervention for cancer therapy[J]. *Acta Pharm Sin B*, 2015, 5: 378–89.
21. Yu TC, Tang B, Sun XY, et al. Development of Inhibitors Targeting Hypoxia-Inducible Factor 1 and 2 for Cancer Therapy[J]. *Yonsei Med J*, 2017, 58: 489–496.
22. Kataria N, Martinez Chloe-Anne, Kerr B, et al. C-Terminal HSP90 Inhibitors Block the HIF-1 Hypoxic Response by Degrading HIF-1 $\alpha$  through the Oxygen-Dependent Degradation Pathway[J]. *Cell Physiol Biochem*, 2019, 53: 480–495.
23. Hubbi Maimon E, Hu Hongxia, Kshitiz, et al. Chaperone-mediated autophagy targets hypoxia-inducible factor-1 $\alpha$  (HIF-1 $\alpha$ ) for lysosomal degradation[J]. *J Biol Chem*, 2013, 288: 10703–14.
24. Naito S, von Eschenbach AC, Giavazzi R, et al. Growth and metastasis of tumor cells isolated from a human renal cell carcinoma implanted into different organs of nude mice[J]. *Cancer Res*, 1986, 46(8):4109–15.
25. Degwert N, Latuske E, Vohwinkel G, et al. Deoxycytidine kinase is downregulated under hypoxic conditions and confers resistance against cytarabine in acute myeloid leukaemia[J]. *Eur J Haematol*, 2016, 97: 239–44.
26. Shuhong Zhou. Effect of Bap on CMA, proliferation, migration and invasiveness of silencing HSP90 $\alpha$  A549 cells[D]. Inner Mongolia Medical University, 2019.
27. Bonam SR, Ruff M, Muller S. HSPA8/HSC70 in Immune Disorders: A Molecular Rheostat that Adjusts Chaperone-Mediated Autophagy Substrates[J]. *Cells*, 2019, 8: undefined.
28. Lappin TR, Lee FS. Update on mutations in the HIF: EPO pathway and their role in erythrocytosis[J]. *Blood Rev*, 2019, 37: 100590.
29. Lacombe C, Mayeux P. The molecular biology of erythropoietin[J]. *Nephrology Dialysis Transplantation*, 1999, 14 Suppl 2(Suppl 2):22–28.
30. Yu T, Tang B, Sun X. Development of Inhibitors Targeting Hypoxia-Inducible Factor 1 and 2 for Cancer Therapy[J]. *Yonsei Med J*, 2017, 58: 489–496.
31. Chan KC, Ting CM, Chan PS, et al. A novel HSP90 inhibitor AT13387 induces senescence in EBV-positive nasopharyngeal carcinoma cells and suppresses tumor formation[J]. *Mol Cancer*, 2013, 12: 128.

## Figures



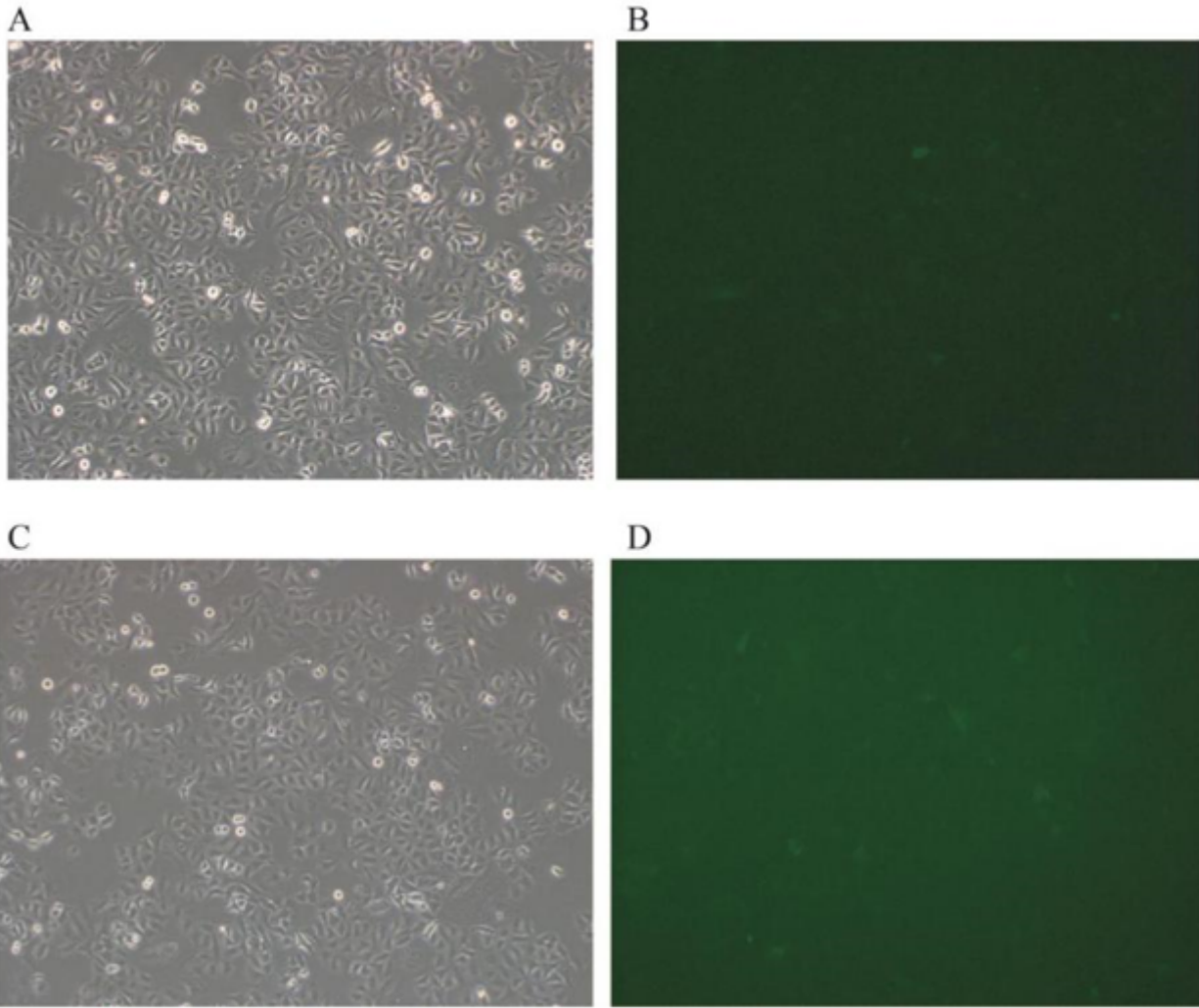


**Figure 1**

Fluorescence expression of cells after lentivirus transfection(100 $\times$ ) (A: white light field diagram of shControl group; B: green fluorescent light field diagram of shControl group; C: white light field diagram of shHSP90 group; D: Green fluorescence field diagram of shHSP90 group)

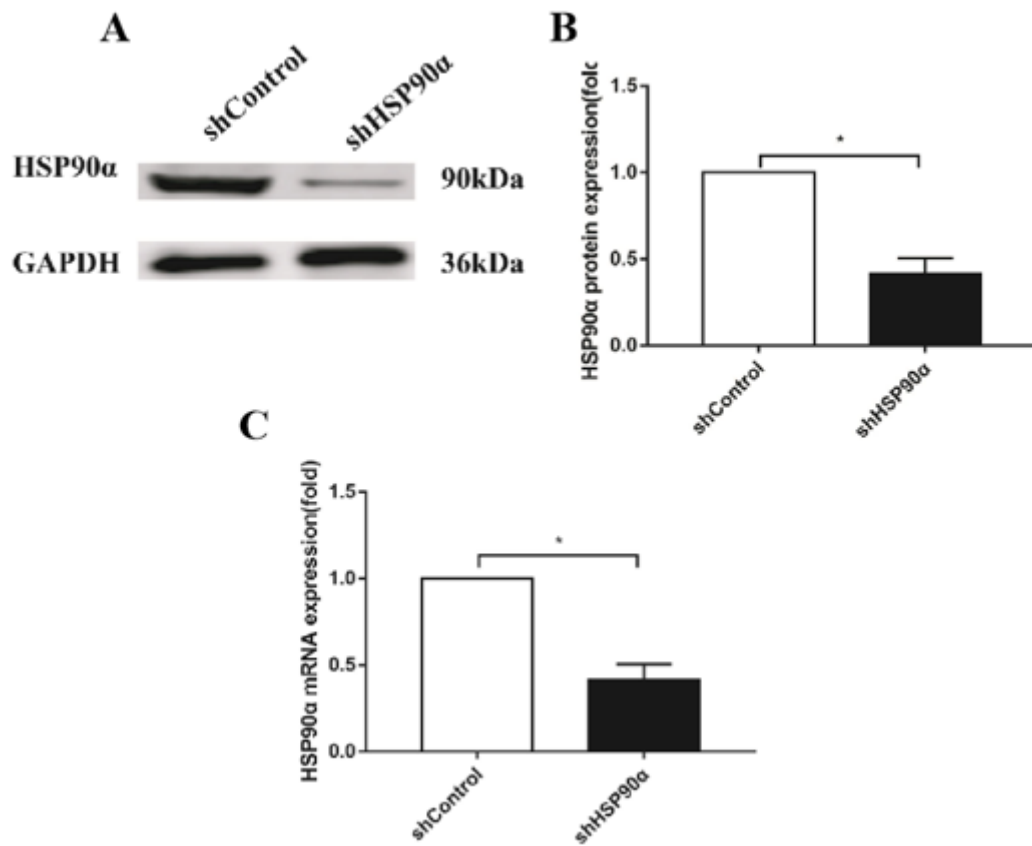
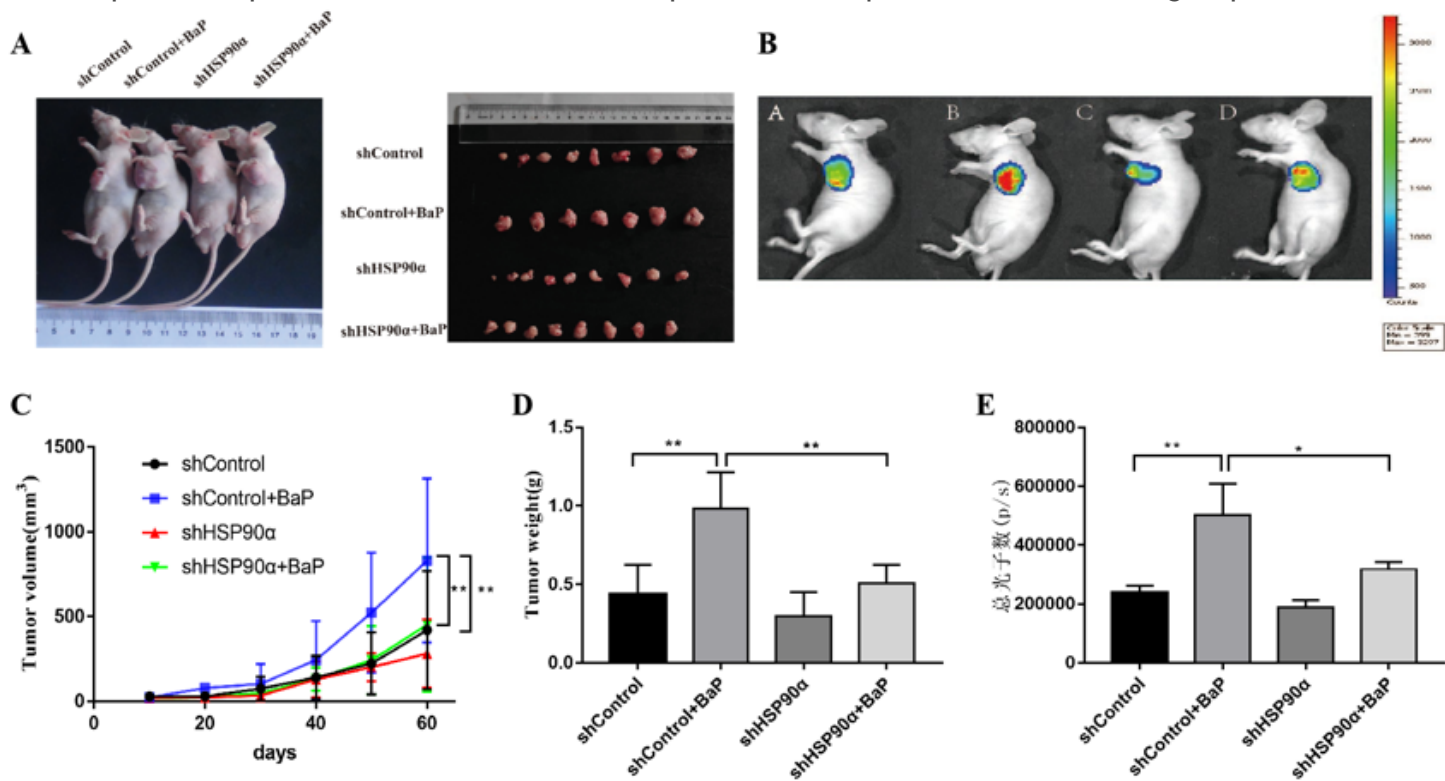


Figure 2

The expression of HSP90 $\alpha$  protein was detected by qPCR and Western blot (A: HSP90 $\alpha$  strip graph; B: HSP90 $\alpha$  protein expression; C: HSP90 $\alpha$  mRNA expression; compared with shControl group, \*P < 0.05, n=3)



**Figure 3**

Tumor formation experiment in nude mice and in vivo imaging of small animals (A: shHSP90 A549 cell transplanted tumor in nude mice; B: shHSP90 A549 cell transplanted tumor in vivo imaging; C: nude mice transplanted tumor growth curve; D: nude mice transplanted tumor body weight chart; E: statistics chart of total photon number of nude mice transplanted tumor in vivo imaging; \*\*P < 0.01, n=10)

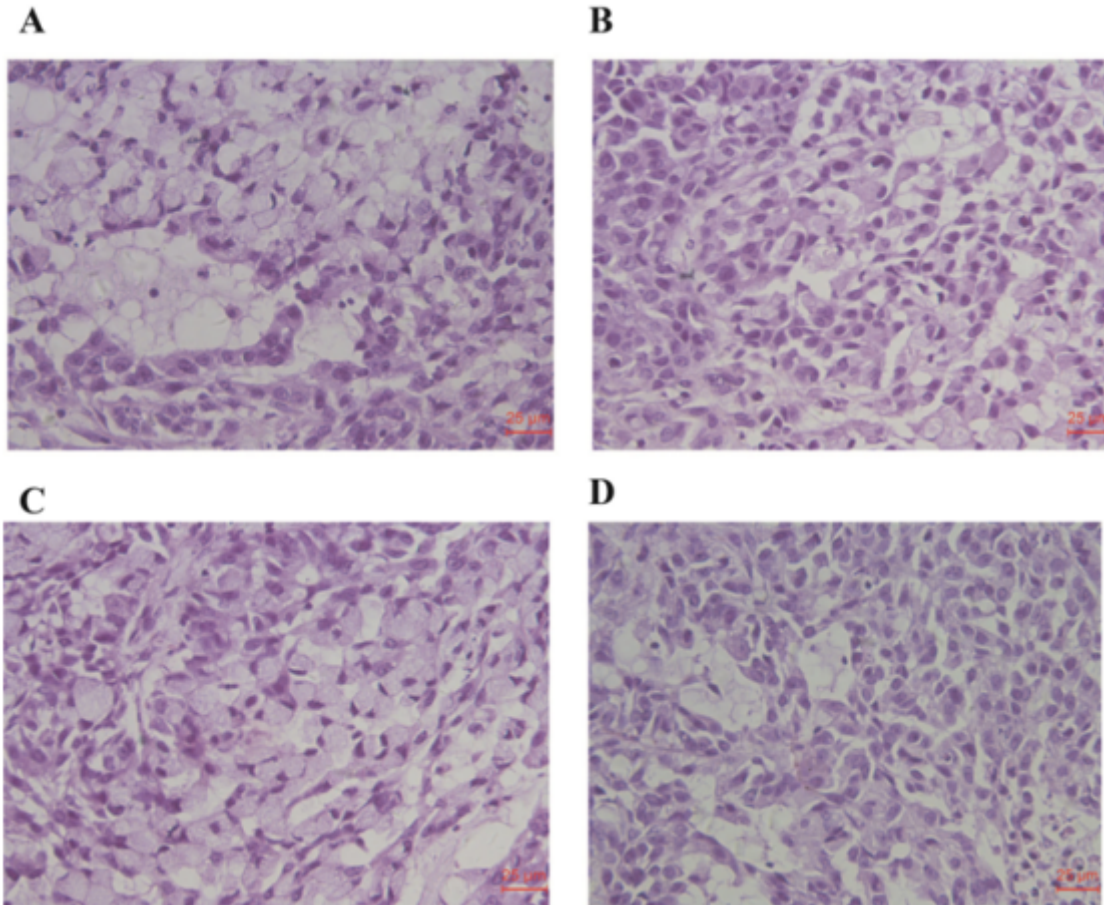


**Figure 4**

The HE staining of the implanted tumor of nude mice of shHSP90 A549 cells (n=10)

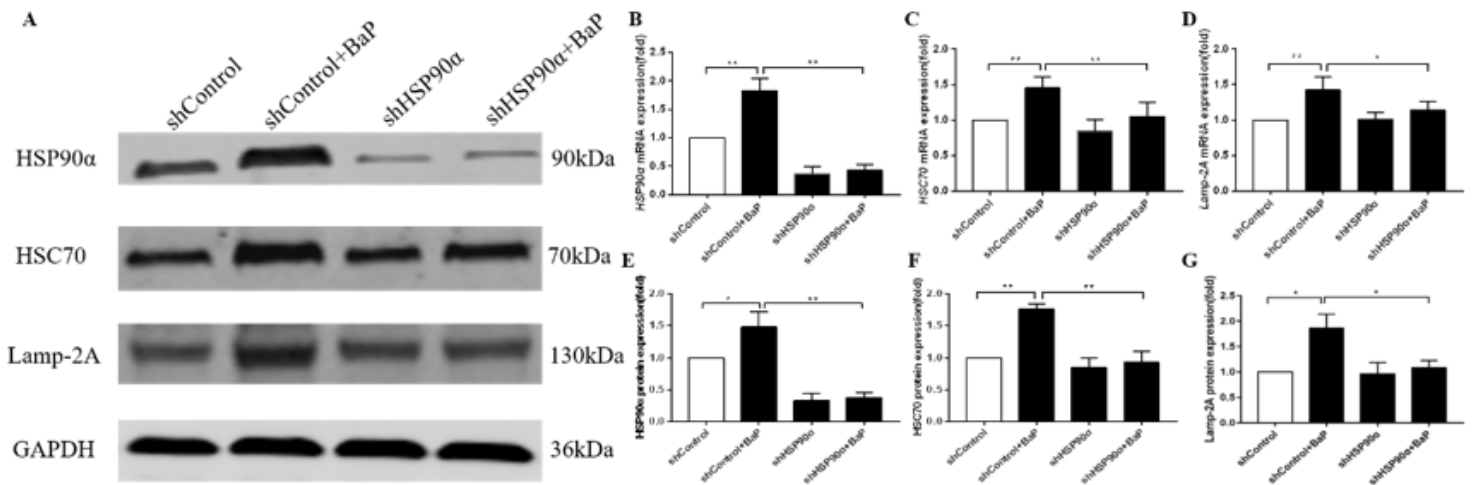




**Figure 5**

The mRNA expression of CMA-related genes of the implanted tumor of nude mice of BaP treated shHSP90 A549 cell (A: Each protein strip graph; B: HSP90 mRNA expression; C: HSC70 mRNA expression; D: Lamp-2A mRNA expression; E: HSP90 protein expression; F: HSC70 protein expression; G: Lamp-2A protein expression; \*P<0.05; \*\*P<0.01; n=10)

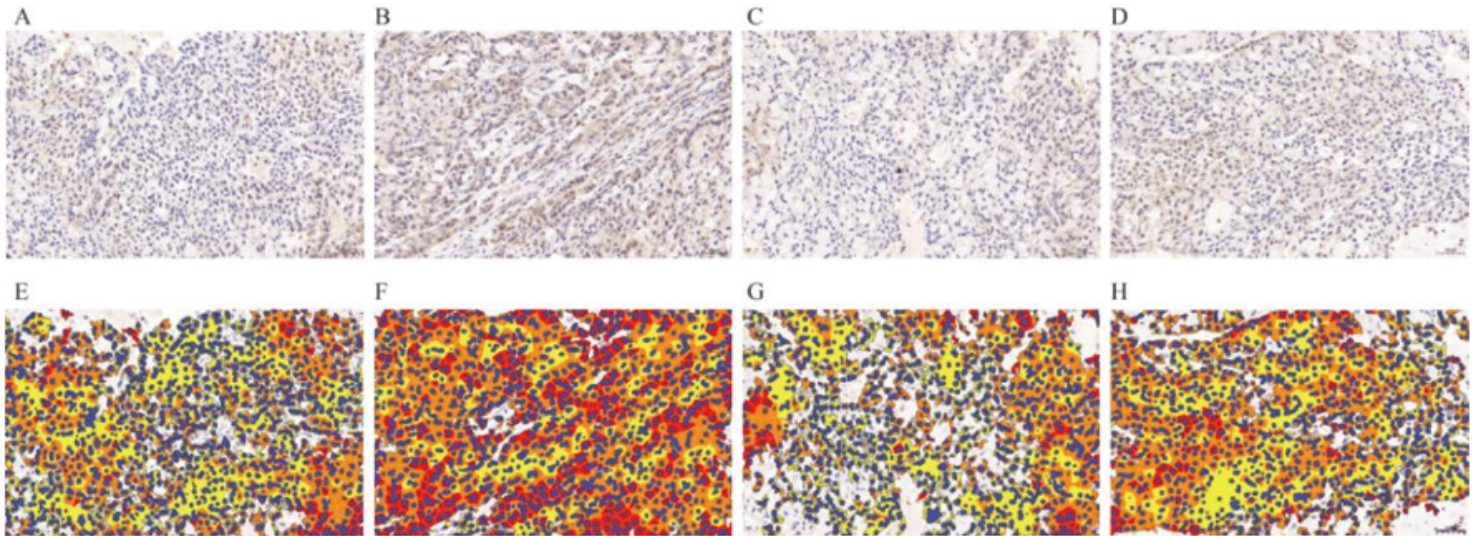


**Figure 6**

Proportion of HSP90 positive degree

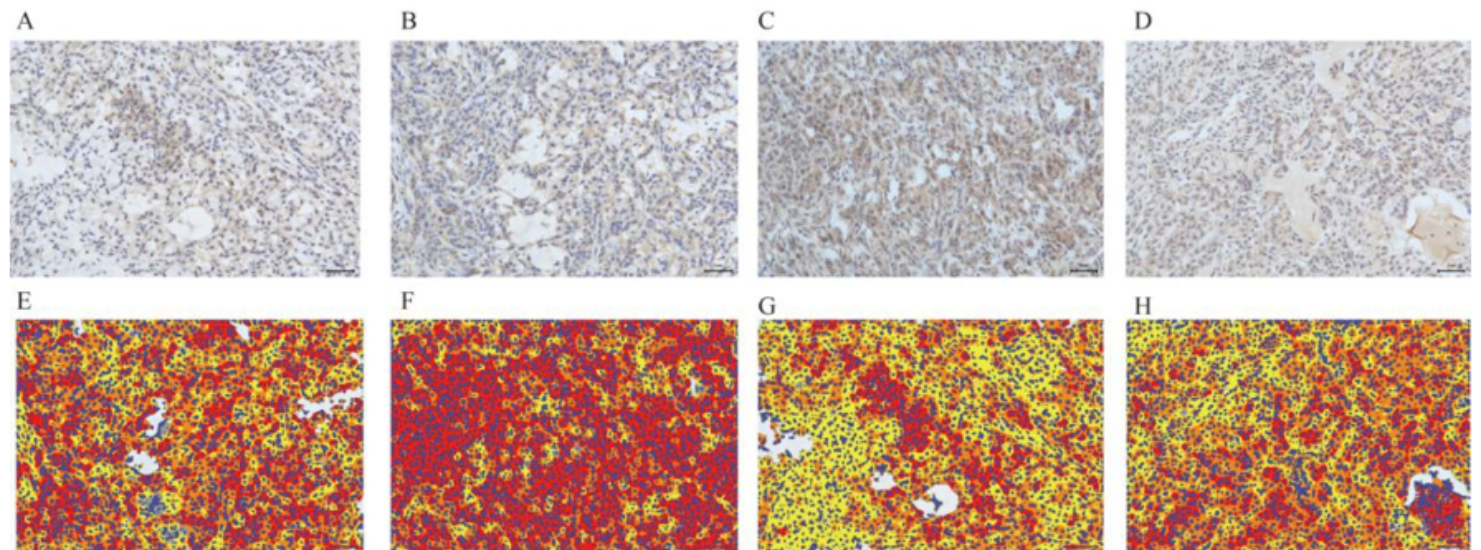


**Figure 7**

Proportion of HSC70 positive degree



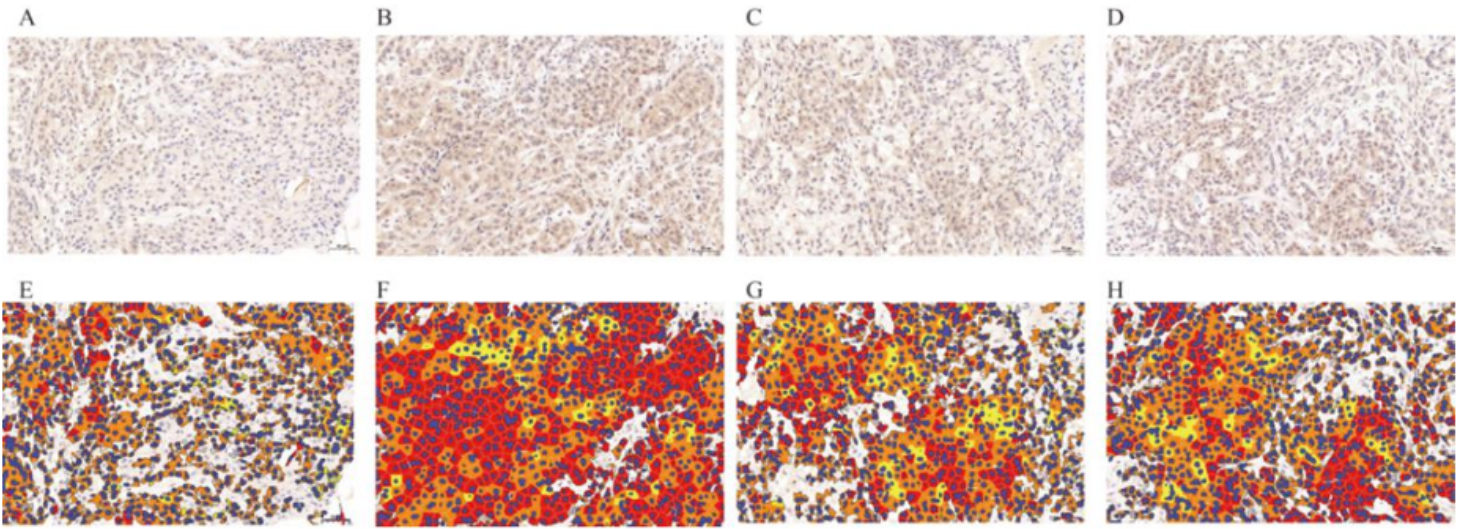


**Figure 8**

Proportion of Lamp-2A positive degree ( A, B, C, D: Immunohistochemical images; E, F, G, H: Immunohistochemical images analyzed by HALO software; A, E: shControl group; B, F: shControl+BaP group; C, G: shHSP90 $\alpha$ ; D, H: shHSP90 $\alpha$ +BaP group; n=10 )

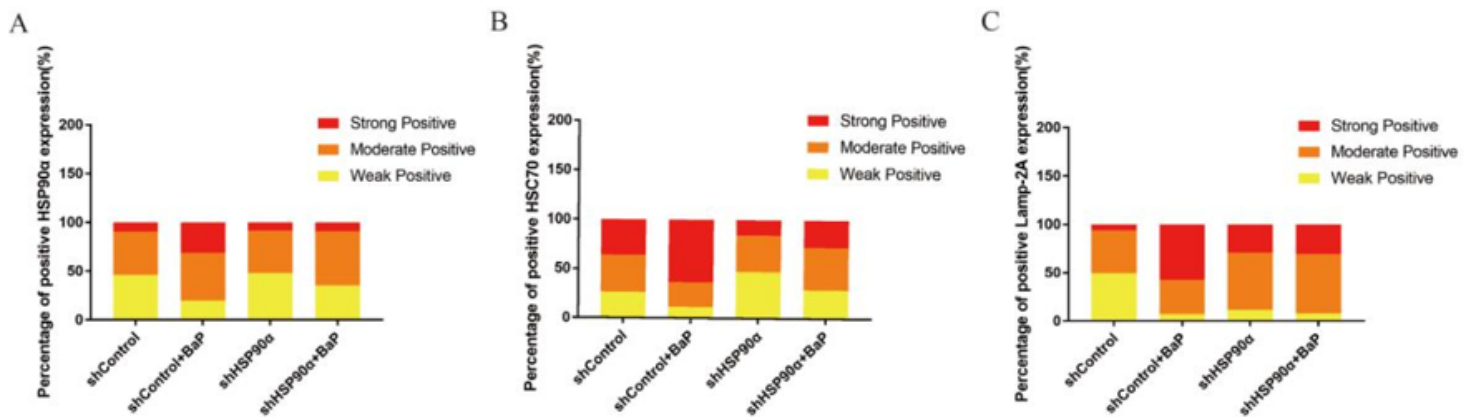


**Figure 9**

Proportion of positive degree of CMA-related protein ( A: HSP90 $\alpha$  protein positive degree statistical graph; B: HSC70 protein positive degree statistical graph; C: Lamp-2A protein positive degree statistical graph )

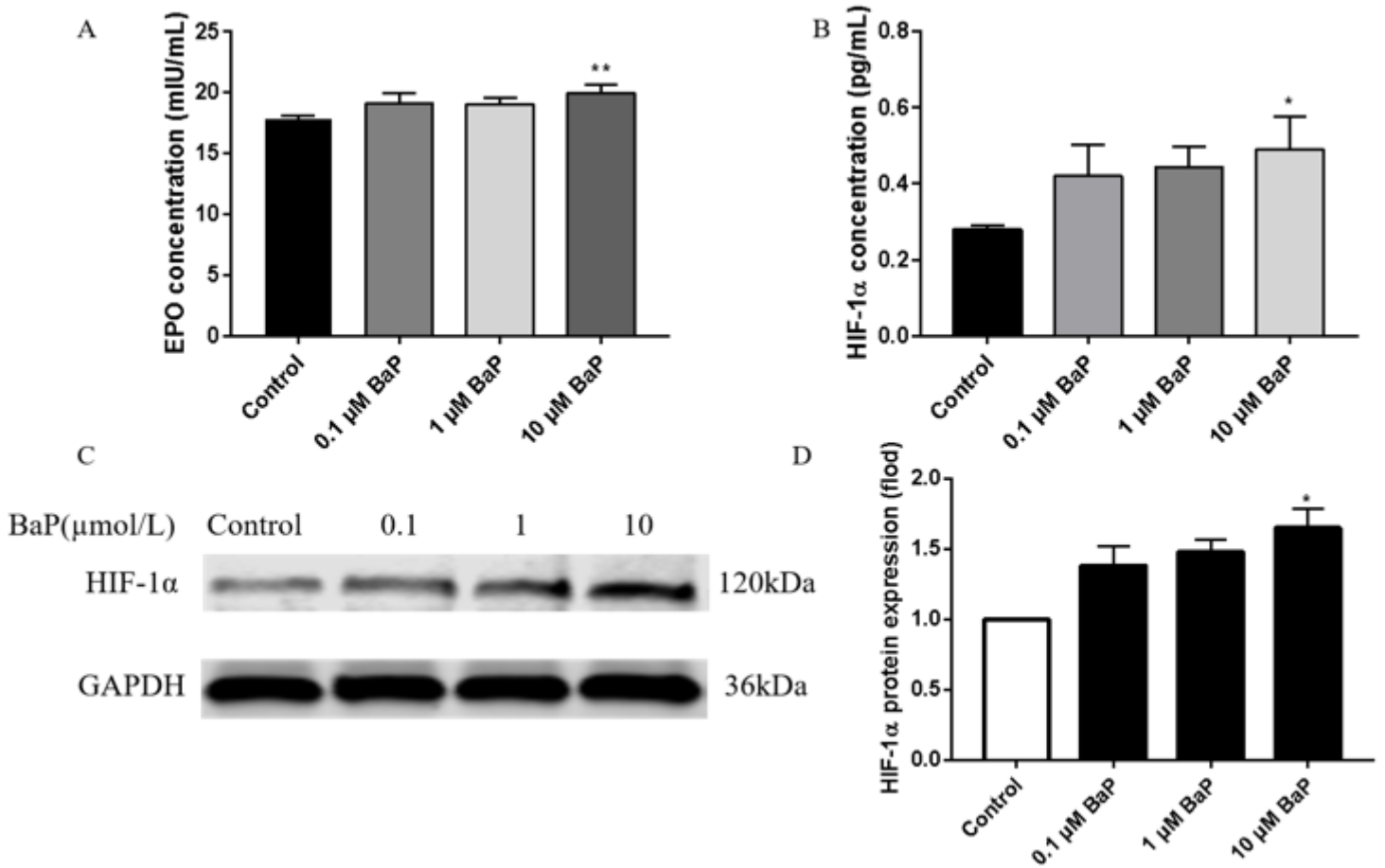


**Figure 10**

The effect of BaP on the concentration of EPO and HIF-1α in A549 cells ( A: The influence of different concentrations of BaP on EPO concentration; B: The influence of different concentrations of BaP on HIF-1α concentration; Compared with Control group, \*means  $P < 0.05$ ; compared with Control group, \*\*means  $P < 0.01$ ,  $n = 3$  )

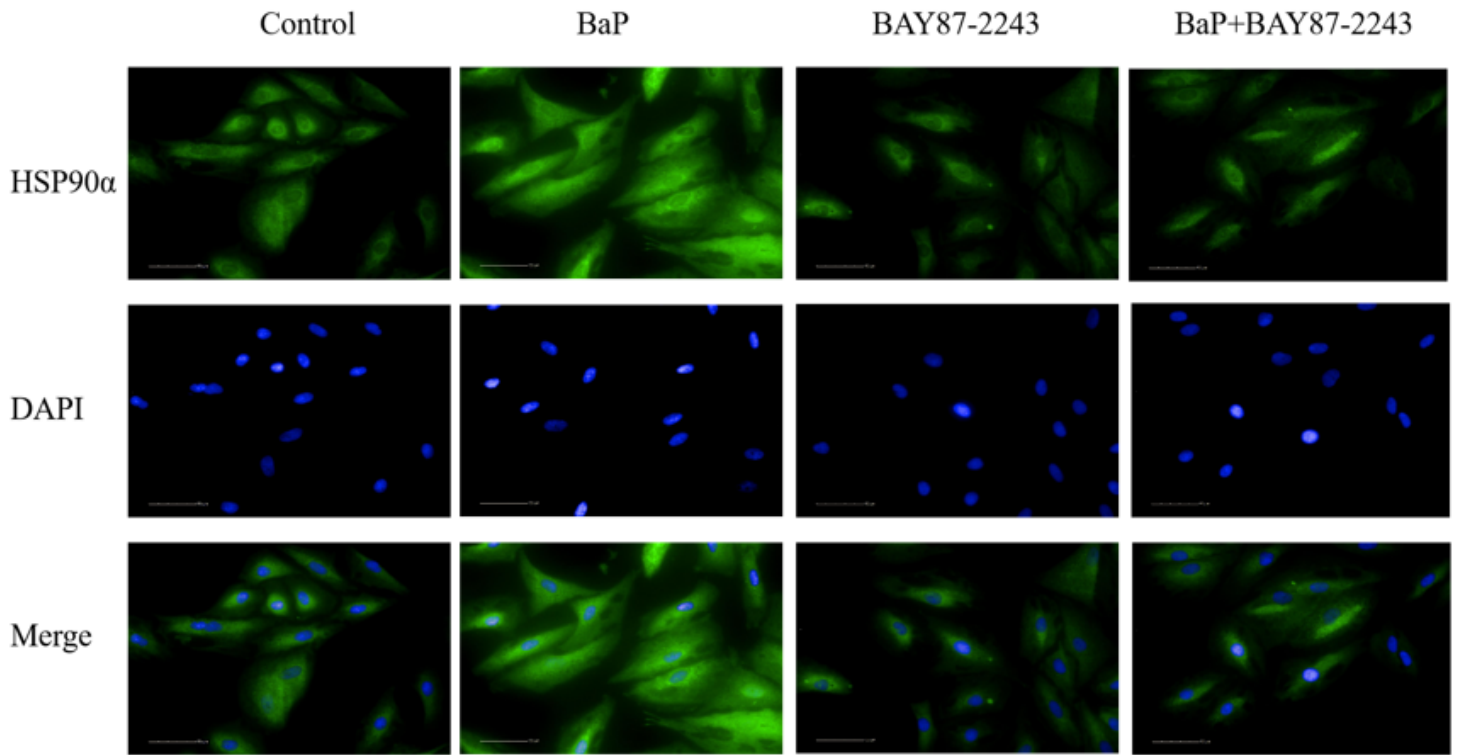


**Figure 11**

HSP90 $\alpha$  protein immunofluorescence (n=3) (Green represents the expression of HSP90 $\alpha$  in A549 cells, blue represents A549 nucleus; n=3)

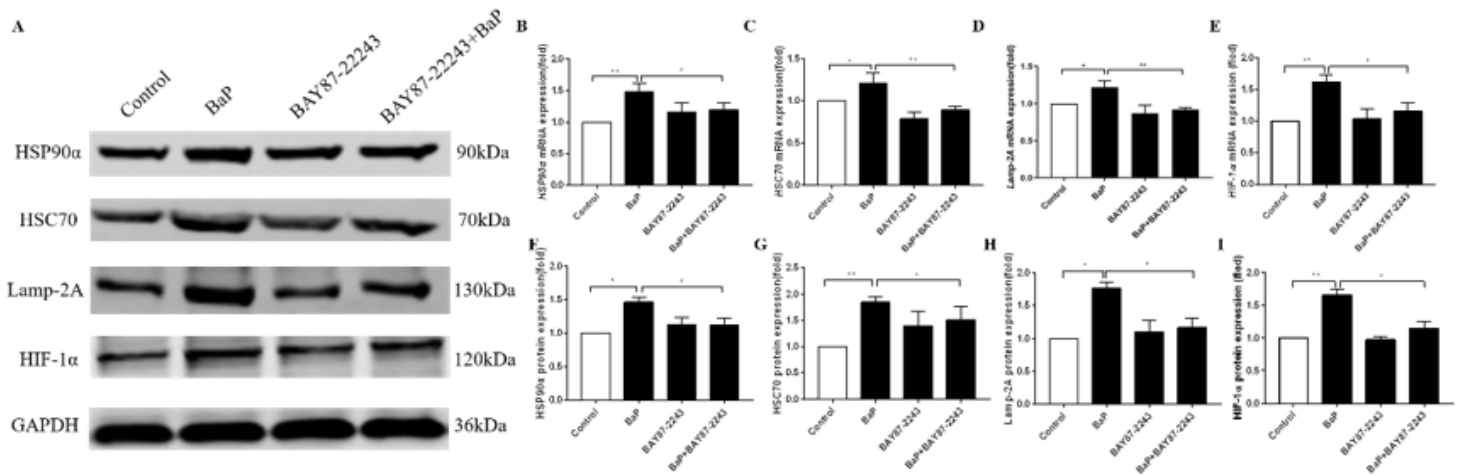


**Figure 12**

HSP90 $\alpha$ , HSC70, Lamp-2A and HIF-1 $\alpha$  mRNA and protein expression (A: Each protein strip graph; B: HSP90 $\alpha$  mRNA expression; C: HSC70 mRNA expression; D: Lamp-2A mRNA expression; E: HIF-1 $\alpha$  mRNA expression; F: HSP90 $\alpha$  protein expression; G: HSC70 protein expression; H: Lamp-2A protein expression; I: HIF-1 $\alpha$  protein expression; compared with the control group, \*P<0.05, \*\*P<0.01, n=3)

## Supplementary Files

This is a list of supplementary files associated with this preprint. Click to download.

- [3.xlsx](#)
- [5.xlsx](#)
- [9.xlsx](#)
- [10.xlsx](#)
- [12.xlsx](#)